

## Optical studies of IV–VI quantum dots

J.L. Machol<sup>a</sup>, F.W. Wise<sup>a</sup>, R. Patel<sup>b</sup>, D.B. Tanner<sup>c</sup>

<sup>a</sup>*Department of Applied Physics, Cornell University, Ithaca, NY 14853, USA*

<sup>b</sup>*Department of Chemistry, Clarkson University, Potsdam, NY 13676, USA*

<sup>c</sup>*Department of Physics, University of Florida, Gainesville, FL 32611, USA*

---

### Abstract

PbS microcrystallites show strong quantum confinement effects on account of the fact that the particle size is much smaller than the exciton Bohr radius, leading to large blue shifts of the optical absorption edge and the transverse optical phonon frequencies. In addition, femtosecond pump-probe experiments find a transient absorption with tetrahertz oscillatory behavior, due to vibrational quantum beats. The frequency of the tetrahertz response agrees with the fundamental infrared absorption of the PbS microcrystallites, suggesting that the vibrational mode to which the photoexcited carriers couple is a transverse optical phonon.

---

### 1. Introduction

In very small semiconducting microcrystallites (or “quantum dots”) one can observe quantum size effects in both linear and nonlinear optical properties [1–3]. These effects occur when the particle size becomes comparable to or smaller than the spatial extent of the wavefunctions of photogenerated electrons or holes, i.e., when the particle radius  $r$  becomes comparable to the carrier Bohr radius,  $a_0 = \epsilon \hbar^2 / 2m^* e^2$ . ( $\epsilon$  is the dielectric constant of the semiconductor and  $m^*$  the effective mass of the electron or hole.) In the semi-conductor materials most studied for quantum size effects, CdS, CdSe, etc., the hole Bohr radius is only  $\sim 10$  Å, so that strong confinement effects are not observed.

Strong confinement effects are more likely in narrow-gap semiconductors, for which  $\epsilon$  and the Bohr radius are large. In this paper we describe optical studies of PbS microcrystallites. These samples had radii of about 20 Å, much smaller than the 90 Å electron or hole Bohr radii. (In terms of volume, the particles themselves only occupy about 1% of the volume associated with the bulk exciton wavefunction [3,4].)

## 2. Experimental details

The PbS microcrystallites were prepared in colloidal solution by arrested precipitation [5]. The colloids, stabilized with poly(vinyl alcohol) (PVA), can be dried to form thin (50  $\mu\text{m}$ ) films consisting of a dispersion of the microcrystallites in the PVA film. From the ratio of Pb to PVA in the starting solution (7.6 mg/1000 mg) the volume fraction of PbS is about 1%. Electron microscopy revealed that the PbS microcrystallites were nearly spherical with average diameters of 43 Å. Electron diffraction showed that the microcrystallites retained the crystal structure and lattice constants of bulk PbS.

The UV/visible absorption of the samples was measured at temperatures between 25 and 300 K using a conventional spectrophotometer. The far-infrared transmission was measured between 15 and 300 K with a Bruker–Fourier spectrometer. In the far-infrared measurements, a stack of 15–20 layers of the thin-film samples was used in order to obtain an adequate absorption; an equal number of PVA layers (without PbS microcrystallites) was used as a reference.

Luminescence measurement were made at 40 K with a cw rhodamine dye laser as excitation source and a Spex double monochromator plus Hamamatsu GaAs PMT to measure the emitted radiation. Far-infrared photoinduced absorption was measured at 15 K with the Bruker interferometer using a cw Argon-ion laser as excitation source.

The  $\sim 100$  fs pulses needed for pump-probe studies were generated by a colliding-pulse mode-locked laser, amplified by a copper-vapor laser amplifier, and converted to white-light continuum in an ethylene glycol jet. Interference filters were used to select wavelength bands between  $\sim 600$  and  $\sim 630$  nm for pump and probe pulses independently. The delay between pump and probe was varied from zero to  $\sim 3$  ps. The ultimate sensitivity of the apparatus is  $\Delta\alpha d \approx 5 \times 10^{-4}$ .

## 3. Results

Fig. 1 shows both the room-temperature absorbance and the photoluminescence of the PbS microcrystallites. Notable are the greatly blue-shifted absorption edge and the series of discrete absorption peaks. Both are due to quantum confinement. The band gap is increased substantially – from 0.41 eV in the bulk to  $\sim 2$  eV in the microcrystallites. The peaks near 600, 390 and 290 nm (2.06, 3.15 and 4.25 eV) can be assigned to the  $1s_e-1s_h$ ,  $1s_e-1p_h/1p_e-1s_h$ , and  $1p_e-1p_h$  exciton transitions, respectively. The best match of the calculated level spacings and the measured excitation energies comes at a particle size of 40 Å, in agreement with electron microscopy. The luminescence peak is red-shifted with respect to the absorption spectrum, suggesting decays to trap states.

Fig. 2 shows the far-infrared transmittance at three temperatures. For all

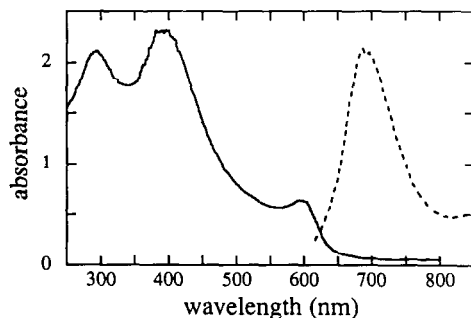


Fig. 1. The solid line shows the 300 K absorbance (arbitrary units) of a sample of the PbS microcrystallites over 250–800 nm ( $40\,000$ – $12\,500\text{ cm}^{-1}$  or  $5$ – $1.5\text{ eV}$ ). The dashed line shows the luminescence intensity spectrum (arbitrary units).

practical purposes, there is no temperature dependence between 15 K and 300 K; the differences among the spectra are likely due to imperfect compensation for the PVA host material and instrumental drift. There are two reproducible features in these data: a strong, broad, asymmetric band centered around  $90\text{ cm}^{-1}$  (11 meV) and a much weaker, sharp feature at  $280\text{ cm}^{-1}$  (35 meV). Neither frequency corresponds to optical phonon frequencies of bulk PbS, which are  $\omega_{\text{TO}} = 65\text{ cm}^{-1}$  (transverse) and  $\omega_{\text{LO}} = 216\text{ cm}^{-1}$  (longitudinal), respectively [6].

Fig. 3 shows the time-dependent nonlinear absorption for three different

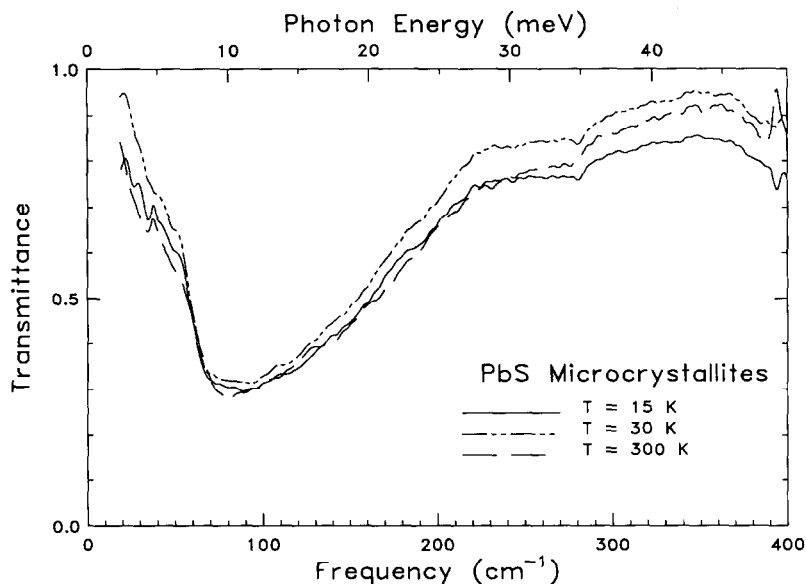


Fig. 2. Ratio of the far-infrared transmittance of PbS microcrystallites in poly(vinyl alcohol) (PVA) to that of PVA alone, is shown for three temperatures.

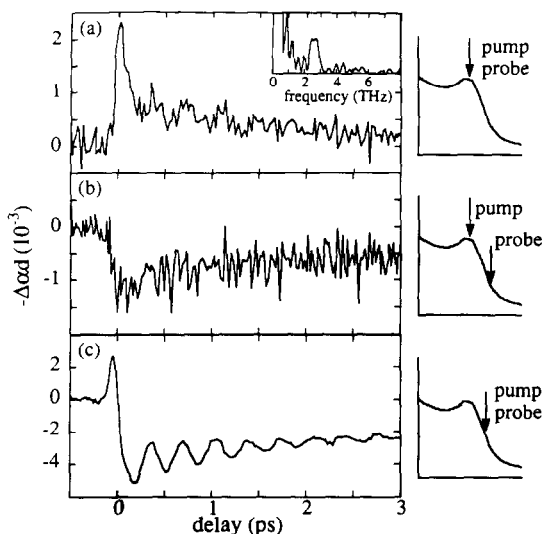


Fig. 3. Time-dependent nonlinear absorption for PbS microcrystallites in poly(vinyl alcohol) for three combinations of pump and probe wavelengths. (a) Pump and probe at 602 nm; (b) pump at 602 nm, probe at 626 nm; (c) pump and probe at 616 nm. The inset to panel (a) shows the Fourier transform of the time signal.

combinations of pump and probe wavelengths. The wavelengths and their relation to the absorbance shown in Fig. 1 are indicated in the little cartoons at the right of each panel. The differences in the signal-to-noise ratios of these data are attributable to differences in output power and stability of the laser system at the different wavelengths. The spike at zero delay in the spectra represents a coherent artifact, which should be disregarded.

In the upper panel, both pump and probe wavelengths (602 nm) coincide with the absorbance maximum; the signal corresponds to a bleaching of the  $1s_e-1s_h$  transition. Superimposed on the recovery signal is an oscillatory term with a period of 385 fs; this component is evident in the Fourier transform of the signal shown in the inset. The frequency of the oscillation is 2.6 THz or  $87\text{ cm}^{-1}$ . The middle panel shows the transient absorption when the pump wavelength (602 nm) is on the resonance while the probe wavelength (626 nm) is at lower energies. In this case there is photoinduced absorption; the low signal/noise ratio makes any oscillations (if they exist) invisible.

The bottom panel shows the case where both pump and probe wavelengths (616 nm) are at lower energies than the absorbance maximum. Here also is photoinduced absorption; superimposed on it is a very obvious oscillatory component. The period of this component is  $\sim 350\text{ fs}$ , corresponding to a frequency of 2.8 THz ( $94\text{ cm}^{-1}$ ).

The change from photoinduced bleaching to photoinduced absorption can be understood in the context of the theory by Hu et al. [7]. Absorption bleaching at

the peak is due to saturation of the  $1s_e-1s_h$  transition. Induced absorption below the peak is due to the formation of a biexciton (two-electron-hole state) via the absorption of one pump and one probe photon. That this absorption is seen when both pump and probe wavelengths are below the peak in the transmission requires some homogeneous broadening of the transition, so that the low energy tail of the exciton transition overlaps the ground-state biexciton transition.

Fig. 4 shows the photoinduced far-infrared absorption,  $-\Delta\mathcal{T}/\mathcal{T} = (\alpha_{\text{photoexcited}} - \alpha_{\text{dark}})d$ , at 15 K, compared to the thermally induced absorption,  $-\Delta\mathcal{T}/\mathcal{T} = [\alpha(30) - \alpha(15)]d$ . The latter quantity has been scaled by a factor of 0.1 to permit comparison with the photoinduced signal. (Note that the convention here is opposite to that in Fig. 3: photoinduced absorption is plotted increasing upwards.)

The photoinduced absorption is extremely reproducible. It consists of a series of narrow-bleaching and induced-absorption peaks spread across the phonon absorption band. Although they appear to be periodic, in fact, they are not. The spacing of features increases from  $20\text{ cm}^{-1}$  near  $70\text{ cm}^{-1}$  to  $28\text{ cm}^{-1}$  by  $150\text{ cm}^{-1}$ .

That the photoinduced features are due to heating cannot be ruled out; some of the photoinduced peaks also appear in the thermal  $-\Delta\mathcal{T}/\mathcal{T}$ . However, some do not, and we speculate that the structure may represent changes of vibrational frequencies in the excited state. This would indicate significant electron-phonon coupling in the PbS microcrystallites.

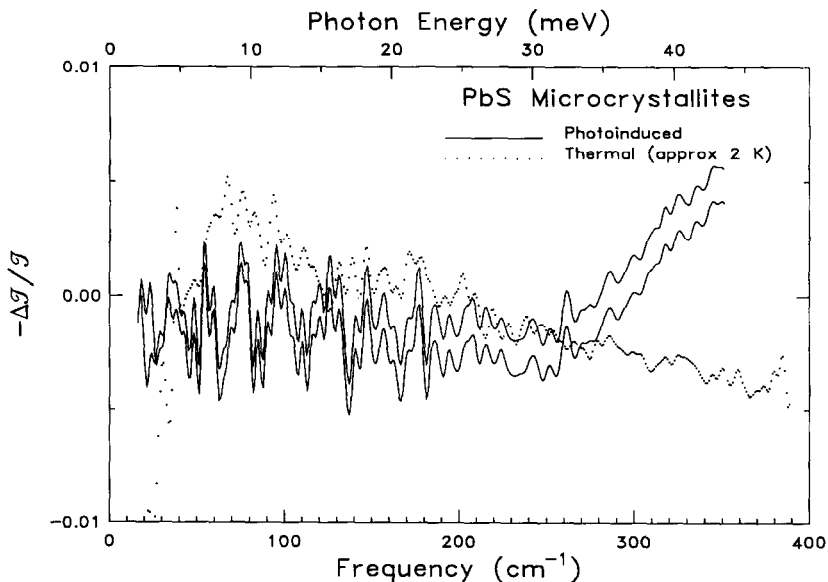


Fig. 4. Solid lines: photoinduced absorption  $-\Delta\mathcal{T}/\mathcal{T} = (\alpha_{\text{photoexcited}} - \alpha_{\text{dark}})d$  for PbS microcrystallites in poly(vinyl alcohol) at 15 K. Dotted line:  $-\Delta\mathcal{T}/\mathcal{T}$  for a temperature change of 10 K, scaled by a factor of 0.2.

#### 4. Discussion

In the remainder of this paper we focus on the far-infrared transmission measurements and their relation to the oscillatory term in the pump-probe measurements. The far-infrared absorption is maximum at  $90 \text{ cm}^{-1}$  (11 meV), a frequency well above the transverse optical phonon of bulk PbS,  $\omega_{\text{TO}} = 65 \text{ cm}^{-1}$ . In small particles, the absorption is expected to be a maximum at the surface optical (SO) phonon or Fröhlich mode, which is the equivalent of the Maxwell–Garnett resonance of an isolated metal particle [8, 9]. For a sphere, the Fröhlich frequency is the solution to  $\epsilon_{\text{particle}}(\omega = \omega_{\text{F}}) = -2\epsilon_{\text{host}}$ , or, using a harmonic oscillator model with a single optical phonon,

$$\omega_{\text{F}}^2 = \omega_{\text{TO}}^2 \frac{\epsilon_{\text{particle}}(0) + 2\epsilon_{\text{host}}}{\epsilon_{\text{particle}}(\infty) + 2\epsilon_{\text{host}}}, \quad (1)$$

where  $\epsilon_{\text{particle}}(\omega)$  is the dielectric function of the PbS microcrystallite and  $\epsilon_{\text{host}}$  is the dielectric function of the host medium, here assumed constant.  $\epsilon_{\text{particle}}(\infty)$  is the dielectric function of the particle at frequencies below the band gap for electronic excitations but well above the LO phonon frequency.

The Lyddane–Sachs–Teller relation,  $\epsilon_{\text{particle}}(0) = \epsilon_{\text{particle}}(\infty)\omega_{\text{LO}}^2/\omega_{\text{TO}}^2$ , allows Eq. (1) to be rewritten as

$$\omega_{\text{F}}^2 = \frac{2\epsilon_{\text{host}}\omega_{\text{TO}}^2 + \epsilon_{\text{particle}}(\infty)\omega_{\text{LO}}^2}{2\epsilon_{\text{host}} + \epsilon_{\text{particle}}(\infty)}. \quad (2)$$

Taking the phonon frequencies and dielectric constants for bulk PbS,  $\omega_{\text{TO}} = 65 \text{ cm}^{-1}$  (transverse),  $\omega_{\text{LO}} = 216 \text{ cm}^{-1}$  (longitudinal) and  $\epsilon_{\text{particle}}(\infty) = 17.2$ , and using  $\epsilon_{\text{host}} = 2.25$ , the SO frequency is  $\omega_{\text{F}} = 205 \text{ cm}^{-1}$ .

In the PbS microcrystallites, the electronic contribution to the dielectric constant will be affected both by changes in electronic band gap and by modifications of the optical oscillator strength. The band-gap widening that we observe will reduce  $\epsilon$ , which would lower the SO frequency. However, as discussed by Schmitt-Rink, Miller and Chemla [10], the oscillator strength for optical transitions is enhanced by small size. Thus the two effects (band gap widening and oscillator strength enhancement) tend to compensate each other. Indeed the details are not important because even if the dielectric constant is reduced to 2, the SO frequency would still be above  $130 \text{ cm}^{-1}$ , considerably to the blue of the observed absorption maximum.

We believe that the far-infrared absorption maximum occurs at the TO phonon frequency, where the frequency has been increased due to the small size of the particles. The lowest frequency vibrational mode that the crystallite can support is one with a wavelength equal to twice the particle radius; with  $r = 20 \text{ Å}$ , the phonon would have a wave vector  $q \approx 2 \times 10^7 \text{ cm}^{-1}$ . Because the TO phonons in PbS have strong dispersion away from the zone center [6], this value of  $q$  in fact corresponds to vibrational frequencies of  $90 \text{ cm}^{-1}$  along both the [001] and [110] directions.

The small size of the particles may also explain why the SO phonon is not observed. Although it is called a “surface” mode, the SO vibration is really due to there being a uniform polarization (dipole moment/unit volume)  $P$  within the particle. The uniform  $P$  leads to a surface charge density, which, in turn, produces a depolarizing electric field within the particle. This field, in the boundary value problem where one calculates the polarizability of the particle when subjected to an external applied field, produces a pole at the SO frequency instead of the TO frequency of the bulk. In a sense, the surface charge density acts to stiffen the mechanical response of the particle. If the particle is mostly surface (as is the case here) this phenomenon may not occur; instead, the response is at the TO frequency.

Finally, we propose that the oscillations occurring in the pump-probe experiment (Fig. 3) are due to quantum beats involving the same TO phonon. The simplest quantum beat phenomenon occurs when there is a three-level system, with two closely-spaced excited states at energies  $\hbar\omega_1$  and  $\hbar\omega_2$ , which are well separated from the ground state. Photoexcitation creates a state which is a coherent superposition of the two excited states and which evolves in time as

$$|a(t)\rangle = \alpha \exp(-i\omega_1 t)|1\rangle + \beta \exp(-i\omega_2 t)|2\rangle, \quad (3)$$

where  $|1\rangle$  and  $|2\rangle$  are the two excited states and the amplitudes  $\alpha$  and  $\beta$  depend on the excitation spectrum and transition probabilities. The relaxation probability then contains modulation terms of the form  $\alpha\beta \cos(\omega_1 - \omega_2)t$ ; it oscillates with a frequency given by the splitting of the two levels.

The beats occur with frequencies in the 2.6–2.8 THz ( $\sim 90 \text{ cm}^{-1}$ ) range, exactly the frequency of the infrared absorption maximum in Fig. 2. Thus, in the data of Fig. 3 we associate  $\omega_2$  with an the  $1s_e-1s_h$  confined exciton and  $\omega_1$  with the same exciton plus one quantum of TO vibrational energy.

In most previous studies where quantum beat phenomena were attributed to vibrational modes, it was the LO phonons that were considered. Here, in contrast, it is the TO mode that is important. The reason for this difference is unclear. It should be noted that in CdSe, where most such effects have been observed [1,2], the TO–LO splitting is only about 15%, and the observed frequency from the pump-probe measurement,  $205 \text{ cm}^{-1}$ , lies between the TO and LO frequencies [11]. In PbS, in contrast, the TO and LO frequencies are separated by almost a factor of four, so there is no doubt that the beat frequency observed is much closer to the TO than the LO frequency.

## Acknowledgements

This work was supported by the National Science Foundation under grant Nos. DMR-8957988 and DMR-9101676 and by the MRL program of the National Science Foundation under DMR-9121645.

**References**

- [1] M.G. Bawendi, W.L. Wilson, L. Rothberg, P.J. Carroll, T.M. Jedju, M.L. Steigerwald and L.E. Brus, *Phys. Rev. Lett.* 65 (1990) 1623.
- [2] R.W. Schoenlein, D.M. Mittleman, J.J. Shiang, A.P. Alivisatos and C.V. Shank, *Phys. Rev. Lett.* 70 (1993) 1014.
- [3] J.L. Machol, F.W. Wise, R.C. Patel and D.B. Tanner, *Phys. Rev. B* 48 (1993) 2819.
- [4] J.L. Machol, Ph.D. Thesis, Cornell University, unpublished.
- [5] M.T. Nenadović, M.I. Comor, V. Vasić and O.I. Mičić, *J. Phys. Chem.* 94 (1990) 6390.
- [6] M.M. Elcombe, *Proc. R. Soc. London A* 300 (1967) 210.
- [7] Y.Z. Hu, M. Lindberg and S.W. Koch, *Phys. Rev. B* 42 (1990) 1713;  
Y.Z. Hu, S.W. Koch, M. Lindberg, N. Peyghambarian, E.L. Pollock and F.F. Abraham, *Phys. Rev. Lett.* 64 (1990) 1805.
- [8] L. Genzel and T.P. Martin, *Surf. Sci.* 34 (1973) 33.
- [9] For a review, see G.L. Carr, S. Perkowitz and D.B. Tanner, in: *Infrared and Millimeter Waves* Vol. 15, K.J. Button, ed. (Academic Press, Orlando, 1984).
- [10] S. Schmitt-Rink, D.A.B. Miller and D.S. Chemla, *Phys. Rev. B* 35 (1987) 8113.
- [11] D.C. Reynolds, C.W. Litton and T.C. Collins, *Phys. Stat. Sol.* 12 (1965) 3.